Deep Learning Based Computationally Efficient Unrolling IAA for Direction-of-Arrival Estimation

Ruxin Zheng†, Hongshan Liu†, Shunqiao Sun† and Jian Li‡

†Department of Electrical and Computer Engineering, The University of Alabama, Tuscaloosa, AL, USA
‡Department of Electrical and Computer Engineering, University of Florida, Gainesville, FL, USA

***Abstract*—We introduce a computationally efficient approach for direction-of-arrival (DOA) estimation in automotive radar systems using a single-snapshot. Classical subspace-based methods like MUSIC and ESPRIT may apply spatial smoothing on uniform linear array to create multiple snapshots for accurate DOA estimation. However, spatial smoothing has the drawback of reducing the array aperture and it is not feasible for sparse linear arrays. The existing single-snapshot-based methods like compressive sensing and iterative adaptation approach (IAA) have high computational costs and slow convergence times, which poses challenges for real-time implementations. While strides in optimization algorithms and hardware acceleration strategies propose plausible remedies to alleviate these constraints, enhancing their appropriateness for real-time use, the computational cost remains notably high. The recent deep learning-based DOA estimation methods have shown good performance in terms of inference time and estimation accuracy, but lack interpretability and generalization. To address these limitations, we propose an unrolling iterative adaptive approach (UAA) that unrolls the IAA algorithm into multiple deep neural network layers. The UAA network has better generalization and avoids the high computational costs associated with matrix inversions. Extensive numerical experiments show that the UAA network outperforms IAA in terms of inference time and estimation accuracy under different signal-to-noise ratio (SNR) scenarios.**

***Index Terms*—Automotive Radar, DOA estimation, Iterative Adaptive Approach, Algorithm Unrolling, Array Signal Processing, Deep Learning**

I. Introduction

Automotive multiple-input multiple-output (MIMO) radars are an essential part of advanced driver assistance systems and self-driving cars, mainly because they are low cost, capable of sensing in bad weather, and unaffected by poor visibility conditions [1]–[6]. Frequency-modulated continuous-wave (FMCW) is commonly used in automotive radar systems with low-cost analog-to-digital converters (ADCs). The targets are separated in range-Doppler domains using two-dimensional fast Fourier transform (FFT), and a constant false alarm rate (CFAR) detector is used to select a subset of range-Doppler bins for direction-of-arrival (DOA) estimation through a third FFT. As a result, current automotive radar only provides sparse point clouds. To improve the angular resolution and generate high-resolution radar images, automotive radar can perform high-resolution DOA estimation for each range-Doppler bin to produce range-azimuth spectra imaging in bird's-eye view format [7]–[10].

The DOA estimation problem has been extensively studied in the literature. The parametric subspace-based high-resolution approaches, such as multiple signal classification (MUSIC) [11] and the estimation of signal parameters via rotational invariance techniques (ESPRIT) [12], [13], require multiple snapshots to obtain an accurate estimation of the array covariance matrix. However, in a highly dynamic automotive environment, it is challenging to have multiple snapshots, and usually only a single-snapshot in available [4]. The single-snapshot MUSIC algorithm was introduced in [14]. It calculates the MUSIC pseudo spectrum using a Hankel matrix constructed from a single-snapshot array response. However, subspace-based approaches suffer from high computational cost, due to singular value decomposition and angle scanning.

Compressive sensing (CS) [15] based sparse sensing techniques have been shown to have super-resolution performance [16] and work well for automotive radar DOA estimation with single-snapshot by exploiting the sparse nature of targets in the angular domain. For CS-based DOA estimation algorithms, it is required that a dictionary satisfies the restricted isometry property (RIP) condition [17], which requires an optimal design of antenna arrays such that the peak sidelobe level is low [4]. Another well-known DOA estimation algorithm that works for single-snapshot is the iterative adaptive approach (IAA) [18], [19] which is an iterative and nonparametric method. IAA has been shown to be robust in DOA estimation compared with CS approach. However, the main challenge of implementation CS and IAA is their high computational costs.

Recently, data-driven deep learning (DL) for DOA estimation has received increasing attention [20]–[22]. In general, DL-based methods have several important advantages over traditional methods, such as fast inference time, enhanced super-resolution capabilities, and performing well at low SNR [20]. Deep learning techniques are mostly data-driven and lack interpretability, while traditional iterative algorithms are more interpretable because they model the physical processes with domain knowledge. Consequently, a technique called algorithm unrolling has recently been proposed and is gaining popularity due to its ability to provide a concrete and systematic link between traditional iterative algorithms and deep neural networks [23]. One of such unrolling network example for sparse signal recovery is the learned iterative shrinkage

This work was supported in part by U.S. National Science Foundation (NSF) under Grant CCF-2153386 and Alabama Transportation Institute (ATI).

thresholding algorithm (ISTA) [24].

In this paper, we present a novel unrolling iterative adaptive approach network (UAA) for single-snapshot DOA estimation. The proposed approach is designed to provide better interpretability compared to conventional deep neural networks by mimicking IAA in an unrolled manner. Through extensive numerical experiments under various signal-to-noise ratio (SNR) scenarios, we demonstrate that UAA outperforms IAA in terms of inference time and DOA estimation accuracy. Additionally, UAA outperforms data-driven DL approaches in terms of its ability to generalize and estimate DOAs that have not been seen before. These results highlight the potential of the UAA as a promising solution to DOA estimation problems with superiority over existing methods in terms of performance and interpretability.

II. System Model

Consider a general linear antenna array of N elements and there are K far-field point targets with angles θ_k for $k = 1, \cdots, K$. The array response can be written as

$$\mathbf{y} = \mathbf{A}(\theta)\mathbf{s} + \mathbf{n}, \tag{1}$$

where $\mathbf{n}$ represents a complex $N \times 1$ white Gaussian noise vector, and $\mathbf{A}(\theta) = [\mathbf{a}(\theta_1), \mathbf{a}(\theta_2), \cdots, \mathbf{a}(\theta_K)]$ is the $N \times K$ array manifold matrix, where

$$\mathbf{a}(\theta) = \left[1, e^{\frac{2\pi d_2}{\lambda}\sin\theta}, \cdots, e^{\frac{2\pi d_N}{\lambda}\sin\theta}\right]^T. \tag{2}$$

Here, d_n is the element spacing between the n-th element and the first element, and $\mathbf{s} = [s_1, s_2, \cdots, s_K]^T$ is the source vector. In this paper, we are interested in estimating the parameter θ, i.e., the target DOAs, using a single-snapshot of the array response $\mathbf{y}$.

IAA is a data-dependent, nonparametric algorithm [18]. The DOA space is discretized into a grid of L points, and the array manifold is defined as $\mathbf{A}(\theta) = [\mathbf{a}(\theta_1), \cdots, \mathbf{a}(\theta_L)]$. The covariance matrix of $\mathbf{y}$ can be represented by $\mathbf{R} = \mathbf{A}(\theta)\mathbf{P}\mathbf{A}^H(\theta)$, where P is a $L \times L$ diagonal matrix with the l-th diagonal element being $P_l = |\hat{s}_l|^2$. Here, $\hat{s}_l$ is the estimate of the source reflection coefficient corresponding to direction θ_l.

IAA iteratively estimates the reflection coefficient $\hat{s}$ and updates the covariance matrix by minimizing the weighted least-square (WLS) cost function $\|\mathbf{y} - s_l\mathbf{a}(\theta_l)\|^2_{\mathbf{Q}^{-1}(\theta_l)}$, where $\|\mathbf{X}\|^2_{\mathbf{Q}^{-1}(\theta_l)} \triangleq \mathbf{X}^H\mathbf{Q}^{-1}(\theta_l)\mathbf{X}$ and the interference and noise covariance matrix $\mathbf{Q}(\theta_l) = \mathbf{R} - P_l\mathbf{a}(\theta_l)\mathbf{a}^H(\theta_l)$. The solution to this optimization problem is

$$\hat{s}_l = \frac{\mathbf{a}^H(\theta_l)\mathbf{R}^{-1}\mathbf{y}}{\mathbf{a}^H(\theta_l)\mathbf{R}^{-1}\mathbf{a}(\theta_l)}. \tag{3}$$

The computational cost of each IAA iteration is $2LM^2 + LM + M^3$, where M is the number of array snapshots and L is the number of discretized grids. Fast IAA algorithms [25]–[27] have been proposed, exploiting the FFT operation and Gohberg-Semencul (GS) representation of the inverse of $\mathbf{R}$. The computational cost of each fast IAA iteration is $M^2 + 12\zeta(2M) + 3\zeta(L)$, where $\zeta(L)$ stands for the computational cost of performing FFT of size L, i.e., $O(L\log L)$ [26]. The superfast IAA uses a conjugate gradient (CG) algorithm to approximate the inverse of $\mathbf{R}$ to further reduce the computational cost. Still, the high computational cost of IAA and the fast IAA algorithms is a bottleneck that prevents their real-time implementation in automotive radar systems.

III. An Unrolling Iterative Adaptive Approach Network For DOA Estimation

In this section, we introduce the unrolling iterative adaptive approach (UAA) network, a novel approach that combines the classical IAA with unrolled deep networks. The UAA generates a pseudo-spectrum, containing estimated reflection coefficients, by scanning a grid. This enables us to formulate the DOA estimation as a spectrum estimation problem, rather than a multi-label classification task.

A. The UAA Architecture

We provide a comprehensive overview of the UAA architecture, highlighting its key components and innovative features. The choice of using a recurrent neural network (RNN), specifically a gated recurrent unit (GRU) [28], is motivated by its ability to efficiently process sequential data, which makes it an ideal choice for array signal processing. The core idea behind UAA is to take the iterative process of IAA and truncate it into discrete steps, which are then mapped to GRU blocks. Each GRU block is composed of two GRUs, GRU-T and GRU-B, which respectively emulates the numerator and denominator of the fraction, $\frac{\mathbf{A}^H(\theta)\mathbf{R}^{-1}\mathbf{y}}{\mathrm{diag}(\mathbf{A}^H(\theta)\mathbf{R}^{-1}\mathbf{A}(\theta))}$, in IAA. The outputs of the GRUs are passed through ReLU and dense layers, which are then concatenated and fed into a final dense layer that performs the division operation to generate the spectrum estimation, $\hat{\mathbf{s}}$. This estimation is then used to update the covariance matrix, $\mathbf{R}$, for the next GRU block.

Turning the iterative solver into a deep neural network with multiple layers results in faster inference compared to traditional model-based optimization. The end-to-end learning of iteration-specific parameters in deep unrolling networks allows for fewer layers to be used to achieve comparable performance [29]. In our implementation, four GRU blocks are employed. The UAA architecture is shown in Fig. 1.

B. Data Generation and Labeling

We use a uniform linear array (ULA) consisting of $N = 20$ elements with inter-element spacing of half-wavelength to generate the simulated beam vectors for maximal 3 targets with DOAs of $\{\theta_k\}$ and a minimum separation of $\Delta\phi = 6°$. The radar field of view (FOV) is set as $\boldsymbol{\phi}_{\mathrm{FOV}} = [-30°, 30°]$, which is discretized with a step size of $1°$, resulting in a grid $\mathbf{g} = [g_1, \cdots, g_M]^T \in \mathbb{R}^{M\times 1}$ with $M = 61$ possible DOA angles. The reflection coefficients s_k for each DOA source are randomly generated complex numbers. The label of the

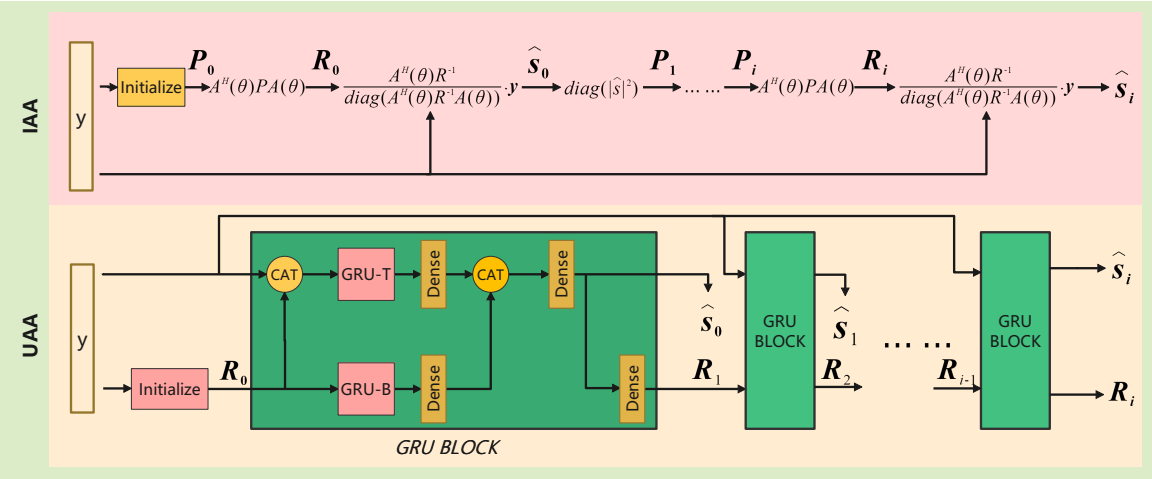

Fig. 1. The illustration of the IAA algorithm (top), and the architecture of UAA (bottom).

beam vector is denoted by $\hat{\mathbf{g}} = [\hat{g}_1, \cdots, \hat{g}_M]^T \in \mathbb{R}^{M\times 1}$, and it can be expressed as

$$\hat{g}_m = \begin{cases} |s_k|, & \text{if } \theta_k = g_m \\ 0, & \text{else} \end{cases} \tag{4}$$

To create the beam vectors, we use a combination of various angles and random reflection coefficients and repeat the process three times. We also add varying levels of noise by sampling the signal-to-noise ratio (SNR) uniformly from a range of 0 dB to 30 dB with increments of 5 dB. The resulting training set consists of $470,946$ beam vectors.

C. Training Approach

The proposed UAA model was trained for 200 epochs with a batch size of 256, using the Adam optimizer with a learning rate of 0.001 and a mean squared error (MSE) loss function. The model was trained end-to-end without any additional pre-processing or post-processing steps. The goal of this training was to minimize the MSE loss and achieve accurate predictions. The experiment was carried out in Python 3.8 using PyTorch 1.10 and CUDA 11.1 on four Nvidia RTX A6000 GPUs. To prevent overfitting, a separate validation set was generated in the same way as the training set, but with different random reflection coefficients. The training and validation loss were carefully monitored and are plotted in Fig. 2. The weight with the lowest validation loss was selected for all performance evaluation tasks in Section IV.

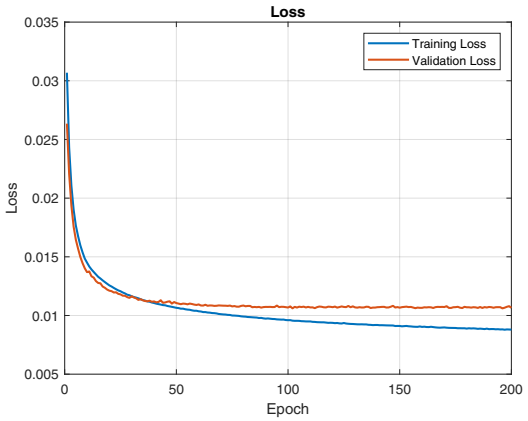

Fig. 2. The training and validation loss of UAA.

IV. Performance Evaluation

We evaluate the UAA model in four crucial aspects of DOA estimation: accuracy, separability, generalizability, and complexity. To provide a comprehensive comparison, the performance of the UAA model is benchmarked against traditional DOA estimation methods, including IAA and digital beamforming (DBF) implemented via FFT, as well as a convolutional neural network (CNN) that has been specifically trained for DOA estimation as a multi-label classification problem on a discrete grid [20]. The CNN proposed in [20] consisted of four two-dimensional (2D) convolution layers and four dense layers. It was originally designed for N_s snapshot, with $N_s \in [100, 10000]$, but it has been adjusted for single-snapshot scenarios in this evaluation. According to [30], IAA exhibits superior performance compared to other prominent sparse signal representation techniques like Sparse Bayesian Learning (SBL). As a result, we have chosen to exclusively employ IAA as our benchmark algorithm for the purpose of our research. The maximum number of iterations for IAA is set to 15, as the performance improvement becomes negligible after around 15 iterations [18]. In addition, under IAA, the FOV $[-30°, 30°]$ has been discretized into the same 61 points as the UAA model for angle scanning. For DBF, the FFT length is set to $N_{\text{DBF}} = 2,048$ to ensure the accuracy of the frequency-domain representation. All experiments are conducted using $5,000$ Monte Carlo trials.

The comparison will provide insights into the strengths and weaknesses of the UAA model in comparison to these widely-used methods, and demonstrate the unique capabilities of the UAA model in single-snapshot DOA estimation.

A. Accuracy

We have selected the root mean squared error (RMSE) as our performance metric to evaluate the accuracy of DOA estimation methods. Our methodology follows the conventional grid-based DOA estimation approach, where a peak search is performed to extract the DOA estimates from the UAA estimated spectrum. For each Monte Carlo trial, an off-grid source with a direction randomly drawn from the interval $[-30°, 30°]$ is generated, along with its corresponding SNR. As demonstrated in Figure 3, the RMSE vs SNR chart shows that the UAA algorithm outperforms CNN across all SNR scenarios, providing comparable high DOA estimation accuracy to IAA for higher SNR (greater than 5dB) and even greater accuracy for lower SNR. The dark dashed line in the chart represents the grid-induced error, which is calculated as the RMSE between the source DOA and its closest angle on the grid. This error serves as a lower bound for this performance metric. It is important to highlight, with fairness in mind, that the DBF method utilized in this particular subsection follows the same grid implementation as the IAA. Moreover, the SNR is defined as the ratio between the power of the signal and the power of the accompanying noise.

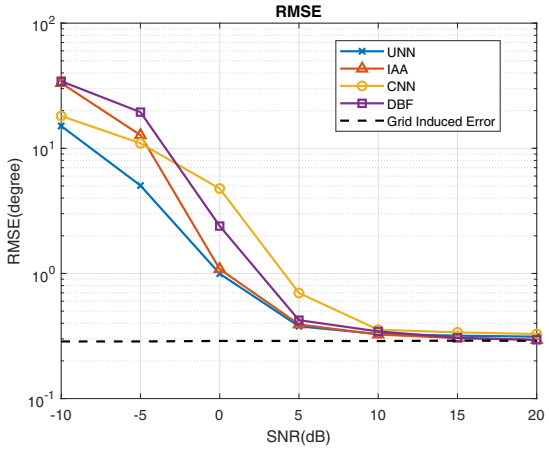

Fig. 3. The logarithmic scale RMSE versus SNR in the DOA estimation of a single, randomly generated off-grid target.

B. Separability

To evaluate the DOA estimation performance in resolving closely located targets, we design an experiment with two targets situated at $-\Delta\theta/2$ and $\Delta\theta/2$, respectively. The $\Delta\theta$ represents the angular distance between the targets. The trial is considered a "hit" if the difference between the estimated DOAs and ground truth falls within $\pm 1°$. The hit rate is calculated as the fraction of successful "hit" trials out of $5,000$ Monte Carlo trials under SNR of 40 dB.

As illustrated in Fig. 4, the IAA demonstrates the ability to resolve targets with an angular separation of $2°$. A comparison between the CNN and UAA reveals that the former slightly outperforms the latter when the target separation is less than $4°$. However, it's important to note that both CNN and UAA were trained on data that only contained targets with a minimum angular separation of $6°$. As a result, their resolution capabilities are limited by the quality of the training data. The 3-dB beamwidth of the tested array's beampattern is around $5.1°$. Therefore, the hit rate of the DBF method increases significantly when the separation between two targets surpasses $6°$.

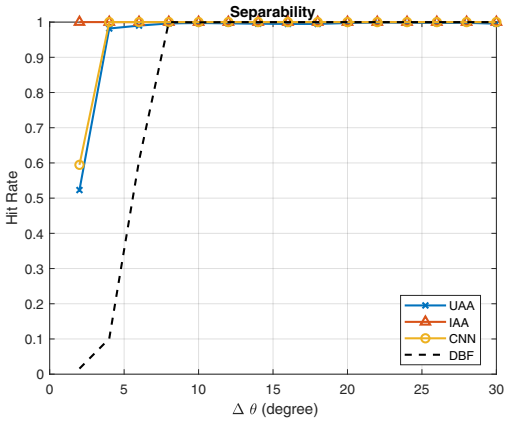

Fig. 4. Performance evaluation of UAA, CNN, DBF, and IAA algorithms: hit rate vs $\Delta\theta$.

C. Generalizability

To further assess the generalizability of both the CNN and the UAA methods, an experiment was conducted using four off-grid targets located at $[-25.2°, -10.6°, 5.3°, 15.1°]$. The test data is generated with varying SNRs and random reflection coefficients, to serve as unseen data.

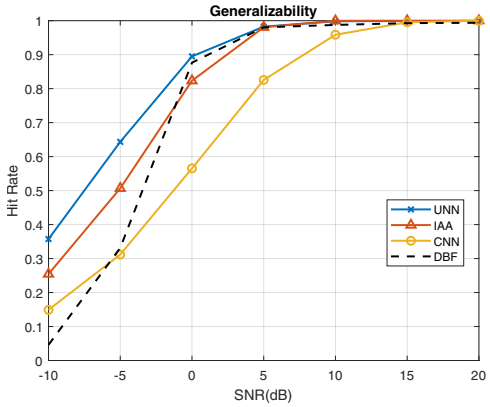

Fig. 5. Performance evaluation of UAA, CNN, DBF, and IAA algorithms: hit rate vs SNR.

The results of the generalizability experiment are depicted in Fig. 5, where the performance of various DOA methods were compared. The hit rate analysis suggests that UAA outperforms all other DOA methods across all SNR levels. This superiority is particularly evident when comparing UAA to the CNN method, as the hit rate of UAA is consistently higher. The superior performance of UAA across different SNRs and target locations highlights its potential for wider applications and real-world use.

D. Complexity

We thoroughly evaluated the complexity of the UAA method by analyzing its inference time and trainable parameters. To ensure fairness, all DOA methods were performed in Python 3.8 using PyTorch 1.10 and CUDA 11.1 on a single Nvidia RTX A6000 GPU, and the inference time was measured by averaging over $5,000$ trials. For the deep learning-based methods, a batch size of 1 was used. The results, shown in Table I, reveal that the DBF method has the fastest inference time. The UAA method was found to be 9 times faster than the IAA method. It's worth noting that the CNN method has a higher number of trainable parameters compared to the UAA method, due to the use of 2D convolution layers, as its input is a 2D covariance matrix. However, the CNN method has a lower inference time than the UAA method, which may be attributed to its fewer layers.

Methods	Inference Time (ms)	# Trainable Parameters
DBF	0.12	–
IAA	49.9	–
CNN	1.0	$49,216,317$
UAA	5.7	$127,4096$

TABLE I
INFERENCE TIME COMPARISON OF DOA METHODS

V. CONCLUSIONS

By leveraging the strengths of both classical IAA methods and recent deep learning-based DOA estimation techniques, the UAA network unrolls the IAA algorithm into multiple deep neural network layers. The proposed UAA method provides an innovative solution for high-resolution angle finding in automotive radars with fast inference time by avoiding the high computational cost of large matrix inversion and better generalization capability than purely data-driven deep learning approaches. The numerical experiments conducted in this paper demonstrate that the UAA network outperforms the IAA method in terms of inference time and estimation accuracy under varying SNR conditions. This new approach offers a promising solution for real-time DOA estimation in automotive radars.

REFERENCES

[1] J. Li and P. Stoica, "MIMO radar with colocated antennas," *IEEE Signal Process. Mag.*, vol. 24, no. 5, pp. 106–114, 2007.

[2] S. Patole, M. Torlak, D. Wang, and M. Ali, "Automotive radars: A review of signal processing techniques," *IEEE Signal Processing Magazine*, vol. 34, no. 2, pp. 22–35, 2017.

[3] F. Engels, P. Heidenreich, A. M. Zoubir, F. K. Jondral, and M. Wintermantel, "Advances in automotive radar: A framework on computationally efficient high-resolution frequency estimation," *IEEE Signal Processing Magazine*, vol. 34, no. 2, pp. 36–46, 2017.

[4] S. Sun, A. P. Petropulu, and H. V. Poor, "MIMO radar for advanced driver-assistance systems and autonomous driving: Advantages and challenges," *IEEE Signal Processing Magazine*, vol. 37, no. 4, pp. 98–117, 2020.

[5] S. Sun and Y. D. Zhang, "4D automotive radar sensing for autonomous vehicles: A sparsity-oriented approach," *IEEE Journal of Selected Topics in Signal Processing*, vol. 15, no. 4, pp. 879–891, 2021.

[6] M. Markel, *Radar for Fully Autonomous Driving*. Boston, MA: Artech House, 2022.

[7] B. Major and et. al., "Vehicle detection with automotive radar using deep learning on range-azimuth-doppler tensors," in *IEEE/CVF International Conference on Computer Vision (CVPR) Workshops*, 2019.

[8] R. Zheng, S. Sun, D. Scharff, and T. Wu, "Spectranet: A high resolution imaging radar deep neural network for autonomous vehicles," in *IEEE Sensor Array and Multichannel Signal Processing Workshop (SAM)*, Trondheim, Norway, June 20-23, 2022.

[9] R. Zheng, S. Sun, H. Liu, and T. Wu, "Time-sensitive and distance-tolerant deep learning-based vehicle detection using high-resolution radar bird's-eye-view images," in *IEEE Radar Conference*, San Antonio, TX, May 1-5, 2023.

[10] ——, "Deep neural networks-enabled vehicle detection using high-resolution automotive radar imaging," *IEEE Transactions on Aerospace and Electronic Systems*, pp. 1–16, 2023.

[11] R. O. Schmidt, *A signal subspace approach to multiple emitter location and spectral estimation*. Stanford University, 1982.

[12] R. Roy and T. Kailath, "ESPRIT - estimation of signal parameters via rotation invariance techniques," *IEEE Trans. Acoust., Speech, Signal Process.*, vol. 17, no. 7, pp. 984–995, 1989.

[13] M. Haardt and J. Nossek, "Unitary ESPRIT: How to obtain increased estimation accuracy with a reduced computational burden," *IEEE Trans. Signal Process.*, vol. 43, no. 5, pp. 1232–1242, 1995.

[14] W. Liao and A. Fannjiang, "MUSIC for single-snapshot spectral estimation: Stability and super-resolution," *Applied and Computational Harmonic Analysis*, vol. 40, no. 1, pp. 33–67, 2016.

[15] D. L. Donoho, "Compressed sensing," *IEEE Transactions on Information Theory*, vol. 52, no. 4, pp. 1289–1306, 2006.

[16] E. Candes and C. Fernandez-Granda, "Towards a mathematical theory of super-resolution," *Communications on Pure and Applied Mathematics*, vol. 67, no. 6, pp. 906–956, 2014.

[17] E. Candès and J. Romberg, "Sparsity and incoherence in compressive sampling," *Inverse problems*, vol. 23, no. 3, p. 969, 2007.

[18] T. Yardibi, J. Li, P. Stoica, M. Xue, and A. Baggeroer, "Source localization and sensing: A nonparametric iterative adaptive approach based on weighted least squares," *IEEE Trans. Aerosp. Electron. Syst.*, vol. 46, no. 1, pp. 425–443, 2010.

[19] W. Roberts, P. Stoica, J. Li, T. Yardibi, and F. Sadjadi, "Iterative adaptive approaches to MIMO radar imaging," *IEEE J. Sel. Topics Signal Process.*, vol. 4, no. 1, pp. 5–20, 2010.

[20] G. K. Papageorgiou, M. Sellathurai, and Y. C. Eldar, "Deep networks for direction-of-arrival estimation in low SNR," *IEEE Transactions on Signal Processing*, vol. 69, pp. 3714–3729, 2021.

[21] J. Fuchs, M. Gardill, M. Lübke, A. Dubey, and F. Lurz, "A machine learning perspective on automotive radar direction of arrival estimation," *IEEE Access*, vol. 10, pp. 6775–6797, 2022.

[22] S. Feintuch, J. Tabrikian, I. Bilik, and H. H. Permuter, "Neural network-based DOA estimation in the presence of non-Gaussian interference," *arXiv preprint arXiv:2301.02856*, 2023.

[23] V. Monga, Y. Li, and Y. C. Eldar, "Algorithm unrolling: Interpretable, efficient deep learning for signal and image processing," *IEEE Signal Processing Magazine*, vol. 38, no. 2, pp. 18–44, 2021.

[24] K. Gregor and Y. LeCun, "Learning fast approximations of sparse coding," in *International Conference on Machine Learning (ICML)*, Haifa, Israel, June 21-24, 2010.

[25] M. Xue, L. Xu, and J. Li, "IAA spectral estimation: Fast implementation using the Gohberg-Semencul factorization," *IEEE Trans. Signal Process.*, vol. 59, no. 7, pp. 3251–3261, 2011.

[26] G. O. Glentis and A. Jakobsson, "Efficient implementation of iterative adaptive approach spectral estimation techniques," *IEEE Trans. Signal Process.*, vol. 59, no. 9, pp. 4154–4167, 2011.

[27] ——, "Superfast approximative implementation of the IAA spectral estimate," *IEEE Trans. Signal Process.*, vol. 60, no. 1, pp. 472–478, 2012.

[28] K. Cho, B. Van Merriënboer, D. Bahdanau, and Y. Bengio, "On the properties of neural machine translation: Encoder-decoder approaches," *arXiv preprint arXiv:1409.1259*, 2014.

[29] N. Shlezinger, Y. C. Eldar, and S. P. Boyd, "Model-based deep learning: On the intersection of deep learning and optimization," *IEEE Access*, vol. 10, pp. 115 384–115 398, 2022.

[30] T. Yardibi, J. Li, and P. Stoica, "Nonparametric and sparse signal representations in array processing via iterative adaptive approaches," in *2008 42nd Asilomar Conference on Signals, Systems and Computers*. IEEE, 2008, pp. 278–282.